Journal of Applied Polymer Science

Preparation and characterization of thermoplastic water-borne polycarbonate-based polyurethane dispersions and cast films

Magdalena Serkis, Rafał Poręba, Jiří Hodan, Jana Kredatusová, Milena Špírková
Institute of Macromolecular Chemistry AS CR, Heyrovsky Sq.2, 162 06 Praha 6, Czech Republic
Correspondence to: M. Špírková (E-mail: spirkova@imc.cas.cz)

ABSTRACT: Stable water-borne polyurethane dispersions (PUDs) were prepared from bifunctional aliphatic polycarbonate-based macrodiol, 2,2-bis(hydroxymethyl)propionic acid (DMPA), 1,6-diisocyanatohexane, 1,4-butanediol (BD), and triethylamine. Water-borne dispersion particles are thus solely formed from self-assembled linear PU chains. Both PUDs and PUD-based films were characterized with regards to the concentration of DMPA (ionic species content) and BD (hard-segment content). Average particle size of PUDs decreased and their long-term stability increased with increasing DMPA and decreasing BD concentration. Functional properties of cast films made from PUDs are substantially influenced by the character of the original colloidal particle dispersions. The swelling behavior of the films, their surface morphology, and mechanical properties are more influenced by DMPA than BD contents. At DMPA concentrations higher than 0.2 mmol g^{-1} of the solid mass of polyurethane, distinct self-organization of individual nanoparticles into fibril-like structures was detected by atomic force microscopy and scanning electron microscopy. PU films made from PUD containing high BD as well as high DMPA concentrations have the best utility properties namely sufficient tensile properties and a very low swelling ability. © 2015 Wiley Periodicals, Inc. J. Appl. Polym. Sci. **2015**, *132*, 42672.

KEYWORDS: films; microscopy; nanoparticles; nanowires and nanocrystals; polyurethanes; structure–property relations

Received 15 April 2015; accepted 28 June 2015
DOI: 10.1002/app.42672

INTRODUCTION

Organic solvent-borne polymer dispersion systems used for surface coatings were widely produced and used in the past.[1,2] However, the evaporation of volatile organic compounds (VOCs) is the main problem for this type of applications. To reduce coating costs and eliminate VOCs to the atmosphere, organic solvents were replaced by water, the most environmentally friendly and cheapest medium.[3–5] Currently, aqueous polyurethanes have successfully filled up the applications areas previously reserved for organic solvent-borne polyurethanes. Because of the excellent adhesion to the substrate surface, high abrasion, and fouling resistance, the water-borne PUDs are now frequently used as flexible coatings for textile, wood, leather, and metal applications.[6–8] The size of the particles is a very important parameter because it controls the range of practical applications. Small particles are desired when a thorough and deep penetration of the dispersion into porous material is necessary. However, when a rapid drying is essential, relatively large particles are preferred.[9]

Water-borne PUDs are relatively complex systems, the behavior of which differ significantly from that of polyurethane elastomers (PUE), even though the basic components (i.e., macrodiol, chain extender, and diisocyanate) are very similar or in some cases the same as for PUE formulations. Unlike the solid PUEs, the water-borne PUDs are typical aqueous colloidal systems. Although all polyurethanes possess a number of highly polar urethane groups, they are basically hydrophobic and therefore they precipitate in water. There are two methods how to improve dispersibility of these materials in aqueous media: (i) using an external emulsifier or (ii) incorporating hydrophilic ionic groups into the polyurethane backbone. The main advantage of ionic group introduction into the polyurethane backbone is better stability of the charged polyurethane dispersions than that of systems containing the external emulsifiers.

The size of PU nanoparticles can be controlled by different factors. It strongly depends on temperature, rate of mixing, soft segment molecular weight, ionic group concentration, and the degree of neutralization.[4,9,10] It has been found that the chain hydrophilicity, which depends mainly on the number of ionic species (either cationic or anionic) in the molecular chain, decisively influences the particle size.[9] The hydrophobicity of the soft segment component[5,11] plays also a role, but its effect is much less pronounced.

Polyurethanes prepared from bifunctional diisocyanates, macrodiols (MD), and chain extenders (low-molecular weight diols) are linear block copolymers composed of soft (SS) and hard

(HS) segments. These products exhibit the thermoplastic behavior and have been used for a long time as elastomeric construction materials and soft coatings.[12] Their pronounced thermoplastic nature allows for easy processing, shaping, and forming by industrial processes like injection molding or extrusion. Also the simplicity of recycling and re-processing (compared to chemically cross-linked PU thermosets, more robust to recycling) belongs to their great benefits. Polyether-, polyester-, or polybutadiene-based macrodiols of MW 1000–5000 are frequently used as the components of soft segment which secure the flexibility of PU chains.[11–14] The hard segments acting as physical cross-linking sites reinforcing the PU chain are formed by the reaction of diisocyanates and low-molecular weight diols. It has been found that PUDs obtained from hydroxyl-based chain extenders are more flexible than those based on the corresponding amine based extender.[15]

Polycarbonate-based (PC) polyols which constitute the soft segments are a relatively new class of materials in the field of polyurethanes.[6,12,13,16–19] They are known to provide good weathering, fungi, and hydrolysis resistance and are at the same time highly biocompatible materials.[16] Until now, just a few studies of polycarbonates used as the soft segment components for the PUD preparation have been published.[6,16–19] However, in all these studies, the multifunctional chain extenders such as ethylenediamine, diethylenetriamine, or hydrazine were used which gave rise to branched or chemically cross-linked polymer structures.[8,17–21]

To our knowledge, no research has been performed on the preparation of thermoplastic water-borne PUDs based on PC macrodiol and bifunctional butane-1,4-diol as chain extender despite the fact that this type of PUs represents very attractive materials. To obtain the linear system, bifunctional butane-1,4-diol (BD), previously commonly applied in preparation of elastomers, was used as a chain extender. For the same reason 1,6-diisocyanatohexane (HDI) was used as a linear, aliphatic isocyanate compound. This choice of reactants secures the synthesis of recyclable PU materials*.

This article deals with the preparation and characterization of thermoplastic water-borne PUDs and cast films made from water-borne PUDs. The effect of polymer composition on the characteristics of the dispersions, mainly on the average particle size and long-term stability, is presented. The relationship between the properties of dispersions and resulting PU films, such as morphology, water absorption resistivity, and mechanical properties, is discussed and based the best candidates for practical use are subsequently selected.

*Unlike PU films made from "classical" thermoplastic PU elastomers, all PU films made from water-borne PUDs are fully soluble in polar solvents (acetone, tetrahydrofuran) at laboratory temperature. Acetone used for recycling of PUDs may be a technical solvent, which reduces the costs of re-processing. Moreover, after water addition into these PU solutions and after organic-solvent removal, PU dispersions in water are re-formed. They can be thus re-used in the same manner as original water-borne PUDs.

EXPERIMENTAL

Materials

Commercially available, aliphatic polycarbonate macrodiol (PC, trademark T4672) with the average molar mass around $M_n \sim 2770$ g mol^{-1} (detected by SEC/GPC) was kindly provided by Asahi Kasei Chemical Corporation, Tokyo, Japan. T4672 consists of butylene, C4 and hexylene, C6 units (C6/C4 molar ratio is 7 : 3) connected by carbonate groups and it is end-capped by hydroxyl groups. For the structure, see Figure 1. 1,6-HDI, butane-1,4-diol (BD), 2,2-bis(hydroxymethyl)propionic acid (DMPA), and triethylamine (TEA) were obtained from Sigma–Aldrich. Dried acetone (max. 0.0075% H_2O) was supplied by Merck KGaA, Darmstadt, Germany. Dibutyltin dilaurate (DBTDL, purchased from Sigma–Aldrich) in the form of the 10 wt % solution in Marcol oil (mixture of liquid saturated hydrocarbons) was used as a catalyst.

Dispersion Synthesis

Because of high viscosity of polycarbonate diol, which was used as the soft segment component, all reaction steps (including pre-polymerization) were performed in acetone solutions. The main difference between our polymerization process and the common procedure based on diamines consists in the fact that the chain extension is performed before the dispersion step. This modification prevents the reaction between unreacted NCO groups and water.[11] In the standard procedure of preparation PUDs based on polycarbonate macrodiols with diamines as chain extenders, the neutralization step is performed prior to chain extension.[18,21] Because we used diol, which is less reactive than diamine, we could perform the reaction with 1,4-butanediol before the neutralization. This type of synthesis was used by Nanda and Wicks,[11] who reported the preparation of PUDs based on polyesters diols and 1,4-butanediol as a chain extender. To minimize the reaction of diisocyanates with water which competes with the reaction of hydroxyl groups from diols and could cause a considerable decrease of PU molecular weight,[9,22] a very dry acetone with water content lower than 0.0075 wt % was used. In addition, the organo-tin catalyst (dibutyltin dilaurate) was used to accelerate the urethane-forming reaction with aliphatic diisocyanates and suppress the side reactions with water even more.[23] The main advantage of acetone is that a relatively low content of DMPA is necessary to produce stable dispersion.[11] The synthesis of PUD consisted of four subsequent steps; pre-polymerization, chain extension, neutralization, and dispersion formation by phase inversion process. A simplified preparation procedure is given in Figure 1.

Polycarbonate macrodiol, DMPA, and acetone were placed into a round bottom 100 cm^3 flask equipped with a magnetic stirrer, condenser, and temperature controller, and thoroughly mixed at room temperature to obtain a homogenous solution and a uniform mixture of monomers. The amount of acetone was in all cases 45 wt % of the total mass of the reaction mixture. Subsequently, HDI and the catalyst (0.05 mol % per mol of NCO groups) were added and mixed at the rate of 700 rpm. Then the reaction proceeded at 60°C for 6 h, until a constant NCO content was achieved (checked by FTIR analysis). To avoid the competitive reaction between hydroxyl groups of BD and water,

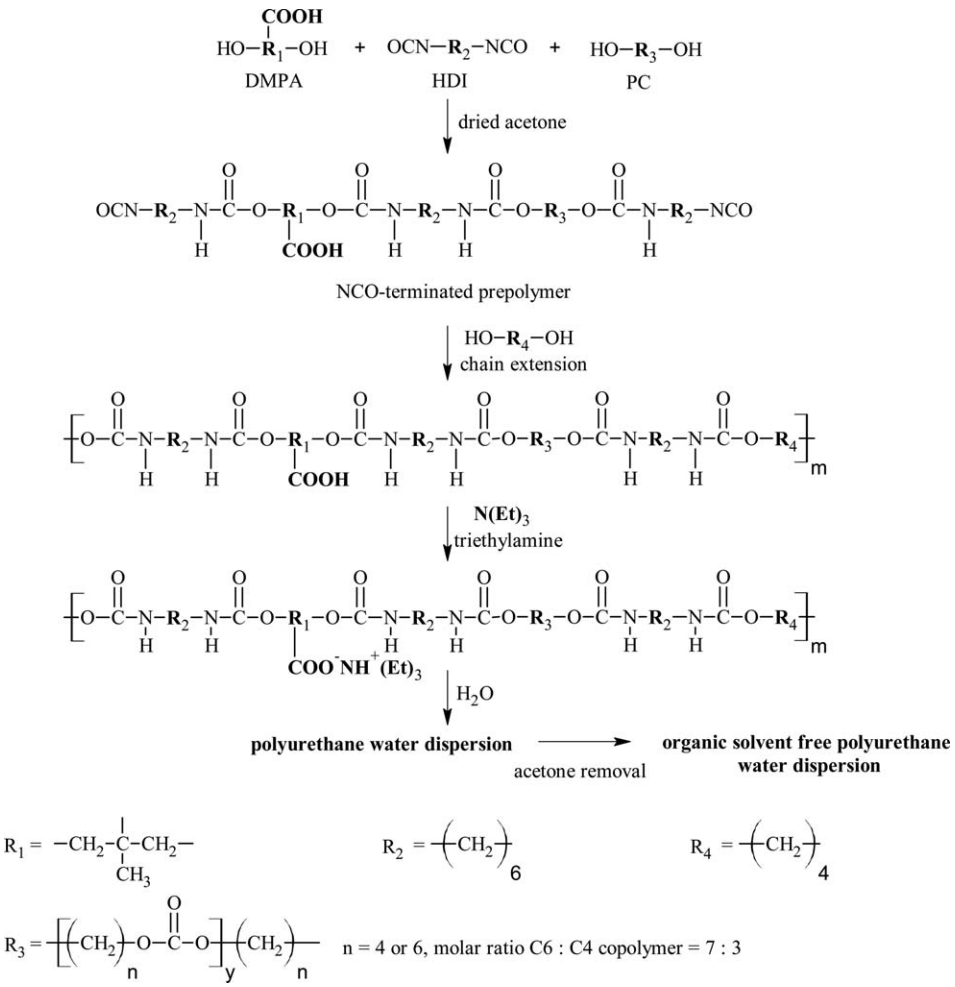

Figure 1. Simplified preparation procedure of the aqueous PU dispersions.

the chain extension reaction preceded the dispersion formation step. The amount of the chain extender (BD in this case) was set to maintain a constant value of the isocyanate index ($r = [NCO]/[OH]_{total} = 1.05$; $[OH]_{total} = [OH]_{PC} + [OH]_{DMPA} + [OH]_{BD}$). The chain extension reaction proceeded for 2 h at 60°C, followed by neutralization of the carboxylic groups by an addition a tertiary amine (TEA) to the polymer solution for 30 min at 55°C, both under constant rate of mixing of 700 rpm. The polymer solution was cooled to room temperature where after water was gradually added with a constant rate of 1 ml min^{-1} using a medical syringe. After acetone removal using rotavap under reduced pressure at room temperature, organic, solvent-free PU water dispersions were obtained. The solid content of polymer in the water dispersion was kept constant in all systems and was equal to 35 wt %.

Film Preparation

All films were prepared by casting the PU dispersions onto Teflon plates followed by slow water evaporation at room temperature for 5 days†. To remove residual water, the films were dried at 50°C for 20 h and subsequently for 1 h at 50°C under vacuum. The final film thickness was controlled by the volume of dispersion used for unit area of the Teflon plate; the final film thickness was in all cases 500 μm ± 25 μm. Obtained films were transparent, they became slightly opaque at increased BD/PC and decreased DMPA/PC ratios.

Methods of Characterization

Gel Permeation Chromatography. The molecular masses, M_n, M_w and polydispersity index, M_w/M_n were determined by gel permeation chromatography (GPC) (Deltachrom pump, Watrex Comp., autosampler Midas, Spark Instruments, two columns with PL gel MIXED-B LS [10 μm]). The eluent was tetrahydrofuran (THF) at flow-rate 0.5 ml min^{-1}. The injection-loop volume was 0.1 ml. Measurements were performed with triple viscosity/concentration/light-scattering detection. The set was connected with a light-scattering photometer DAWN DSP-F (Wyatt Technology) measuring at 18 angles of observation, a modified differential viscometer Viscotek model TDA 301 (without internal light scattering and concentration detectors) and a differential refractometer Shodex RI 71. The data were processed by the Astra and triSEC softwares.

†A modified procedure, that is, film preparation at 50°C immediately after dispersion casting led to deteriorated surface characteristics. For details, see Figure 6 in Surface Analysis of PU Films Prepared by PUD Casting section.

Dynamic Light Scattering. Dynamic light scattering (DLS) measurements were performed using an ALV CGE laser goniometer consisting of a 22 mW HeNe linear polarized laser operating at a wavelength of 632.8 nm, an ALV 6010 correlator, and a pair of avalanche photodiodes operating in pseudo cross-correlation mode. The samples were loaded into 10 mm diameter glass cells and maintained at 25 ± 1°C. Data were collected using ALV Correlator Control software and the counting time of 30 s. To avoid multiple light scattering, all samples were diluted 100 times before measurement.[24] The measured intensity correlation functions $g_2(t)$ were analyzed using REPES algorithm (incorporated in the GENDIST program)[25] giving the distributions of relaxation times shown in equal area representation as $\tau A(\tau)$. The mean relaxation time or relaxation frequency ($\Gamma = \tau^{-1}$) is related to the diffusion coefficient (D) of the nanoparticles as $D = D = \frac{\Gamma}{q^2}$ where $q = \frac{4\pi n \sin(\theta/2)}{\lambda}$ is the scattering vector, n is the refractive index of the solvent, and Θ is the scattering angle. The hydrodynamic diameter (D_H) or the distributions of D_H were calculated[26] using the well-known Stokes–Einstein relation:

$$D_H = \frac{k_B T}{3\pi\eta\ D}$$

where k_B is the Boltzmann constant, T is the absolute temperature, and η is the viscosity of the solvent.

Electrophoretic Light Scattering. Electrophoretic light scattering (ELS) measurements were used to determine the average zeta potentials (ζ) of the nanoparticles using the Zetasizer NanoZS instrument (Malvern Instruments, UK). The equipment measures electrophoretic mobility (U_E) and converts each value to ζ-potential (mV) using Henry's equation:

$$\zeta = \frac{3\eta\ U_E}{2\ \epsilon\ f(ka)}$$

where ε is the dielectric constant of the medium. The parameter $f(ka)$ is the Henry's function which has been calculated through Smoluchowski approximation $f(ka) = 1.5$. The measurements were performed at 25 ± 1°C and each reported ζ-potential value is the average of 10 subsequent measurements.

Differential Scanning Calorimetry. Thermal behavior was measured by Pekin-Elmer DSC 8500 calorimeter with nitrogen purge gas (20 cm^3 min^{-1}). Indium was used as a standard to calibrate the instrument for temperature and heat flow. About 10 mg of each sample was encapsulated in hermetic aluminum pan. Differential scanning calorimetry (DSC) was performed in a cycle heating–cooling–heating from −80°C to 200°C at 10°C min^{-1}. Before and after each of the ramps two minutes of isothermal plateaux were inserted.

Swelling. Swelling experiments were performed at room temperature by immersing the specimens of dry cast films (~0.3 g) into deionized water for the overall time of 16 weeks. The swelling degree was expressed in percentage of the mass increase and calculated according to the equation:

$$\%\ \text{swelling} = \frac{w - w_0}{w} \times 100\ \%$$

where w_0 is the initial weight of the dry film and w is the weight of film in the swollen state.

The percentage weight loss Δw is the weight difference between the weights of dry films before and after swelling, original w_0 and final w_f calculated according to the equation:

$$\Delta w = \frac{w_0 - w_f}{w_0} \times 100\ \%$$

Atomic Force Microscopy. Investigation of the topography and heterogeneity relief of PU films was conducted by atomic force microscopy (Dimension Icon, Bruker), equipped with an SSS-NCL probe (Super Sharp Silicon™—SPM-Sensor from Nano-Sensors™ Switzerland with spring constant 35 N m^{-1} and resonant frequency ≈170 kHz). To investigate PU nanoparticles a freshly peeled out mica (flogopite, $KMg_3(Si_3Al)O_{10}(OH)_2$) surface was covered by dilute water PUD solution (c = ~1 mg ml^{-1}). After water evaporation, the samples were dried in a vacuum oven at ambient temperature for 12 h. The measurements were performed under ambient conditions using tapping mode atomic force microscopy (AFM) technique. The scans covered the sizes from 1 × 1 to 50 × 50 μm^2.

Scanning Electron Microscopy. The microstructure of the films was measured by scanning electron microscopy (SEM) using Vega Plus TS 5135 from Tescan, Czech Republic. Before SEM analysis, the films were sputtered with 4 nm Pt layer using vacuum sputter coater SCD 050 (Balzers, Czech Republic).

Tensile Tests. Tensile properties of the cast films were measured using an Instron model 5800 (Instron Limited, UK) according to test method ISO 527 at room temperature with a cross-head speed of 10 mm min^{-1}. The specimens were prepared according to given standard procedure ISO 527-2/5B. The used dimensions of each specimen were: length 35 mm, length and width of the narrowed part: 12 and 2 mm, and thickness 0.5 mm. Mechanical characteristics such as Young modulus E, stress-at-break σ_b and elongation-at-break ε_b were obtained from the tensile curves. Toughness was expressed as the energy to break the sample per volume unit. Reported values were the averages of at least five measurements. Presented tensile curves were taken from the measurements closest to each calculated average value.

RESULTS AND DISCUSSION

Stable water-borne PU dispersions composed exclusively of linear aliphatic chains have been prepared and characterized. The effect of composition (DMPA and BD contents) on the average particle size and ζ-potential, that is, on characteristics that reflect and pre-determine the long-term stability of PUDs, and on their functional properties such as water-absorption resistivity, surface morphology, and tensile properties of the cast PU films made from PUDs have been investigated and discussed.

For a smooth discussion, all samples are marked by codes. The code consists of three letters: either PUD (which stands for polyurethane dispersion), or PUF (which means polyurethane film cast from the relevant PUD). The letter code is followed by two numbers. The first gives the BD-to-PC molar ratio and the

Table I. Sample Codes and Composition of PU Dispersions

Code PUD[a] A–B	BD (mmol g^{-1})[b]	DMPA (mmol g^{-1})[b]	PC (mmol g^{-1})[b]	HDI (mmol g^{-1})[b]	TEA (mmol g^{-1})[b]
PUD 2.5-1	0.74	0.31	0.29	1.40	0.31
PUD 2-1	0.61	0.32	0.31	1.31	0.31
PUD 1-1	0.34	0.34	0.33	1.08	0.35
PUD 0.8-1	0.27	0.35	0.34	1.04	0.36
PUD 0.5-1	0.17	0.36	0.35	0.94	0.36
PUD 0.5-0.4	0.19	0.16	0.38	0.79	0.15
PUD 0.5-0.2	0.20	0.08	0.40	0.72	0.09

[a] PUF A–B: identification of film prepared from PUD of given composition A = BD/PC; B = DMPA/PC.
[b] Concentration expressed per gram of the solid mass of polymer.

second indicates the DMPA-to-PC molar ratio. As mentioned above, two parameters controlling PU compositions were varied and therefore two series of samples with either constant ionic group content (DMPA) or short diol (BD) content were prepared. Sample codes and compositions are given in Table I, in first to sixth column. Because the BD and HDI products contain groups which can form hydrogen bonds, the variation of BD content allow for the regulation of the number of physical crosslinks.[13] Conversely, polymer hydrophilicity of PUDs is controlled by the number of ionic species derived from the DMPA component. From this point of view, the series of PUDs and PUFs with constant ratio DMPA-to-PC (second number) shows the dependence of PU samples on the hard-segment contents while the series with constant BD-to-PC (first number) depicts the dependence of PUD or PUF samples on the contents of ionic groups.

Molecular Weights of Synthesized PUs

The molecular weights were determined by GPC. Dry samples were dissolved in THF in concentration 1 mg cm^{-3}. The results, based on the polystyrene calibration, are listed in Table II. The M_n values of samples containing various BD concentrations (PUD A-1 series) are similar. It is obvious that different amounts of DMPA influence M_n. Decreasing DMPA concentration leads to higher M_n.

Average Particle Size and Long-Term Stability of PUD

Particle size of PU dispersions is a result of the complex processes influenced by reaction conditions such as temperature, rate of mixing, type and concentration of ionic group and chain extender, type of macrodiol and diisocyanate, and the degree of neutralization of the ionic groups. The dispersions are formed by step-wise PU chain polymerization followed by a self-assembly of individual PU chains into the nanometer-size formations in the dispersion step. The complex chemistry of the preparation process requires that the reaction conditions suitable for the reproducible preparation of PUDs with desired functional properties have to be found and optimized. To tune the reaction conditions, FTIR was used to determine the minimum time necessary for the total isocyanate group conversion in the pre-polymerization and chain-extension reaction steps.

Table II. Molecular Weights of Prepared PUDs

Code	M_n (kg mol^{-1})	M_w (kg mol^{-1})	M_w/M_n
PUD 2.5-1	15.3	29.8	1.95
PUD 2-1	12.5	28.4	2.27
PUD 1-1	11.9	27.3	2.30
PUD 0.8-1	12. 2	28.5	2.34
PUD 0.5-1	12.9	30.5	2.36
PUD 0.5-0.4	22.7	48.2	2.12
PUD 0.5-0.2	28.9	58.1	2.01

After the study and validation of all individual steps, the process of the reproducible PUD preparation was set as follows: (i) pre-polymerization for 4 h at 60°C, (ii) chain-extension for 2 h at 60°C, (iii) neutralization for 0.5 h at 55°C, and (iv) finally a 30 min dispersion process at 55°C. All consecutive steps were conducted under stirring at the constant speed of 700 rpm.

The study of the influence of PUD composition on the average size of the nanoparticles was performed for samples with fully neutralized carboxylic groups with triethylamine to suppress complicating polyelectrolyte effects at low ionic strength.[5] As the conditions of preparation were identical for all PUD samples, the differences in average particle size and ζ-potential detected by the dynamic and ELS analyses are due to differences in PUD compositions. The effect of BD concentration (the series PUD A-1, with constant DMPA-to PC ratio) and the DMPA concentration (the series PUD 0.5-B, with constant BD-to-PC ratio) on the *z*-average particle size and on ζ-potential of the samples is presented in Figure 2.

The results are in accordance with literature data[27] and show that the average particle size decreases considerably with increasing DMPA content. The main reason consists in increased solubility of considerably charged polyelectrolyte chains rich in DMPA, that shifts the self-assembly towards dissociation and formation of smaller associates. Two general effects control the solubility of polyelectrolyte chains. The first one is entropic and reflects the increase in translational entropy of counterions, which are released in bulk aqueous medium.[28] The second effect is caused by changes in the solvation and in water structure after the dissociation and ion pairs and separation of individual ions. Both $-COO^-$ and $NH^+(C_2H_5)_3$ are large, so called "water structure-breaking" ionic groups and hence the changes in their solvation lead to the decrease of the

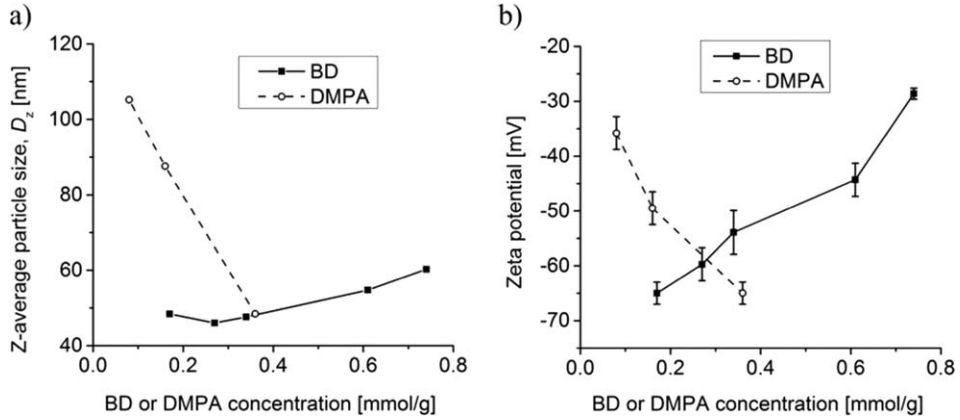

Figure 2. The influence of BD and DMPA concentrations on the *z*-average particle size (left) and ζ-potential (right). BD and DMPA concentration values are given in Table I, second and third column.

Gibbs function of the system.[29] One more effect contributes to the dissociation of particles with increasing DPMA content. The number of ionized —COO^- groups in associates formed by DMPA-rich samples is high and the electric charges are relatively close to each other. Therefore, the electrostatic repulsion is strong, which promotes the dissociation of associates. However, the effect is more complex. The charge of multiply ionized and relatively small nanoparticles (i.e., small for the total bare charge) is in a large extent compensated by counterions which "condense" on charged nanoparticles and lose their translational entropy. In summary, the dissociation of charged polyelectrolyte associates is due in main part to complex entropy reasons.[28] One more (quite trivial) factor contributes to the dependence of sizes of self-assembled nanoparticles on the DPMA content. Data in Table II show that molecular weights of single chains that in aqueous media self-assemble in nanoparticles depend on chemical composition and appreciably increase with decreasing DPMA content. The data further show that the average particle size increases with higher chain stiffness[5] which grows with increasing BD concentrations. This understandable effect is, of course less pronounced (45–60 nm; series PUD A-1) than that of DMPA (48–105 nm; the series PUD 0.5-B). In summary, the number of ionic species affects the self-assembly more significantly than the content of hard segments [for details see Figure 2(a) and Table III].

The values of ζ-potential reflect the efficiency the electrostatic stabilization of dispersed particles in polar liquids (particularly in aqueous media) and control the long-term stability of prepared dispersions[‡]. It is generally accepted that particle suspensions are stable if the absolute value of ζ-potential exceeds 30 mV (i.e., more positive than +30 mV or more negative than −30 mV).[30,31] All prepared PUDs which contain pendant anionic groups in DMPA units exhibit negative ζ-potentials. The influence of the content of ionic groups (DMPA) and hard segments (BD) on the ζ-potential is shown in Figure 2(b). As expected, the content of DMPA strongly influences absolute values of ζ-potential, which increases with increasing DMPA content. It is noteworthy, that the ζ-potential decreases considerably with BD content. This is caused mainly by the fact that the size of self-assembled particles increases with increasing content of BD (as explained above) and hence the charge spreads on a larger surface and the surface charge density is lower as compared with compact particles formed by PUs, which are poor in BD.

As almost all absolute values of ζ-potential are higher than 30 mV, the dispersion can be considered as long-term stable, which was proven experimentally by the stability tests, that is, by storing them at laboratory temperature (23 ± 2°C) for more than 1 year. All dispersions, with the only exception, which was the sample PUD 2.5–1 containing the highest amount of BD, with the value—(29 ± 1) mV, remained stable for more than 1 year. The stability of PUD 2.5–1 was limited and the particles spontaneously coagulated in 5 months.

To summarize this part, the stable water-borne dispersions (formed exclusively by linear PU chains) with *z*-average particle size between 45 and 105 nm were prepared using butane-1,4-diol as the chain extender and 2,2-bis(hydroxymethyl)propionic acid as the anionic species. Increasing DMPA concentration

Table III. Sample Codes, *z*-Average Particle Size, Size-Dispersity Index (PDI), and ζ-Potential of PU Dispersions

Code PUD A-B	*z*-Average particle size, D_z (nm)	PDI[a]	ζ-Potential (mV)
PUD 2.5-1	60.2 ± 0.5	0.20	− (29 ± 1)
PUD 2-1	54.7 ± 1.3	0.29	− (44 ± 3)
PUD 1-1	47.6 ± 0.4	0.13	− (54 ± 4)
PUD 0.8-1	46.0 ± 0.5	0.07	− (60 ± 3)
PUD 0.5-1	48.4 ± 0.2	0.09	− (65 ± 2)
PUD 0.5-0.4	87.6 ± 0.7	0.06	− (50 ± 3)
PUD 0.5-0.2	105.2 ± 10	0.26	− (36 ± 3)

[a] Size-dispersity index was estimated using the cumulant analysis of the autocorrelation functions.

[‡]The system is stable when the repulsive forces between the particles are sufficient enough to overcome their attraction and thus prevent their aggregation. Insufficient number of the ionic species will results in particle aggregation and subsequent sedimentation.

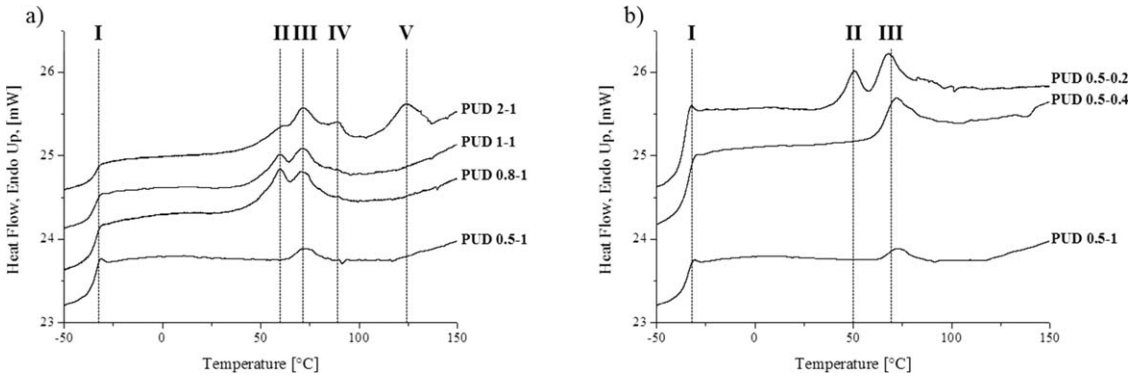

Figure 3. The DSC curves of PUDs-based films containing: (a) various amount of BD, (b) various amount of DMPA. Temperature regions I–V are drawn by the dotted lines.

Table IV. Thermal Properties of PUDs Based Films

Code	HSC_{BD}[a] (wt %)	HSC_{DMPA}[b] (wt %)	T_g[c] (°C)	T_r[d] (°C)	$(T_m)_s$[e] (°C)	$(\Delta H_m)_s$[f] (J g^{-1})
PUD 2-1	16.9	10.0	−34	61	71	11
PUD 1-1	9.6	11.0	−34	60	71	8
PUD 0.8-1	7.6	11.3	−34	60	73	8
PUD 0.5-1	5.2	11.6	−35	-	73	1
PUD 0.5-0.4	5.9	4.9	−34	-	71	4
PUD 0.5-0.2	5.6	2.5	−36	51	67	7

[a] HSC_{BD}—hard segment content derived from BD = $(m_{HDI\ used\ for\ BD} + m_{BD})/(m_{HDI} + m_{BD} + m_{PC} + m_{DMPA}) \times 100$.
[b] HSC_{DMPA}—hard segment content derived from DMPA = $(m_{HDI\ used\ for\ DMPA} + m_{BD})/(m_{HDI} + m_{BD} + m_{PC} + m_{DMPA}) \times 100$.
[c] T_g—glass transition temperature of the soft segments.
[d] T_r—relaxation temperature of the soft segments.
[e] $(T_m)_s$—melting temperature of the soft segments.
[f] $(\Delta H_m)_s$—melting enthalpy of the soft segment.

results in smaller and more stable water dispersions while increasing BD concentration leads to slightly larger and less stable dispersions. The synthesized PU dispersions exhibit suitable functional properties and can be used for preparation of free-standing films, coatings, or adhesives. In this study, the first possibility, that is, the use of stable water PUDs as starting materials for the preparation of cast free-standing PU films was addressed. The chapters of the article that follow focus on results obtained by the characterization and analyses of PU films. At the end of this paragraph, we would like to emphasize that while the behavior of charged PU chains and associates in aqueous media corresponds to the polyelectrolyte regime, in next parts of the study, the thermo-mechanical behavior of bulk films reflects the properties of materials in the ionomer regime.[28] It is why we use the term polyelectrolyte in the beginning of the article and ionomer in the later parts.

Differential Scanning Calorimetry

To investigate the thermal behavior of PUDs, such as melting and organization of crystalline domains, DSC measurements were performed. Row data and the effects of the soft and hard segment content are shown in Figure 3, the thermodynamic characteristics evaluated from DSC curves are listed in Table IV. The DSC thermograms generally show one glass transition temperature (I) at around −34°C and four endothermic peaks (II–V). The second (II) and third (III) peaks at temperatures between 51 and 73°C reflect the thermal behavior of soft segments. The second endothermic region (II) is related to relaxation of the soft segments in the interphase, whereas the third peak (III) is attributed to the melting of highly organized (crystalline) parts formed by the soft phase. The positions of both peaks do not change at relatively high BD content [Figure 3(a)]. It means that the physical cross-links do not significantly affect the motion of soft segments. The intensities of the endotherm peaks are the highest for the BD and DMPA ratios close to 1 (PUD 0.8–1 and PUD 1–1). The difference is visible for the sample with the lowest BD and simultaneously the highest DMPA amount (PUD 0.5–1), where the peak II disappears and intensity of the peak III is the weakest. This is probably due to the fact that BD content approaches the low limit, below which the interaction of ionic groups from DMPA dominates over the effect of hydrogen bonds formed by BD units. It suggests that presence of ionic groups hinders the motion chains[32] and crystallization of PC[§]. The same trend is observed in Figure 3(b) presenting samples from series PUF 0.5-B. The melting enthalpy values of soft segments $(\Delta H)_m$ in region

[§] Auxiliary DSC experiments of model PUs prepared without any BD revealed that endothermic peak III systematically diminished (or even disappeared) if DMPA content gradually increased.

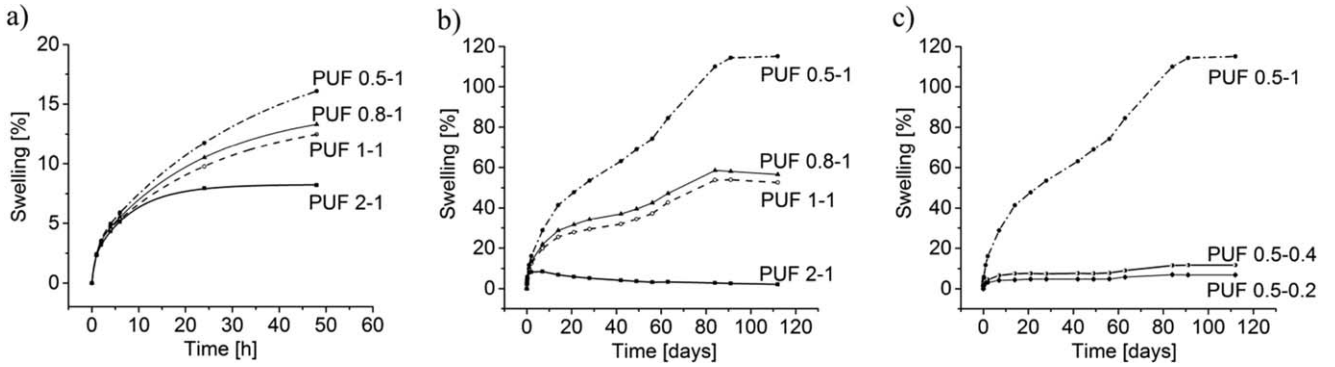

Figure 4. The effect of BD (PUF A-1 series: a, b) and DMPA concentrations (PUF 0.5-B series, c) on swelling properties. Time dependence of the swelling (a) for time up to 50 h, and (b,c) for time up to 16 weeks.

III increase with decreasing DMPA content and indicate better arrangement of chains poor in DMPA.

Multiple melting peaks IV and V at temperatures higher than 85°C occur only for the sample containing the highest HSC_{BD} value (PUD 2–1). They can be attributed either to the presence of highly organized hard-segment domains present in the different crystalline forms[13] or they can be associated with the mixing transition of the soft and hard segments.[33]

Swelling Behavior

The sensitivity and resistivity of cast PU films against water is a paramount criterion for most coating or adhesive applications.[1] The swellability of cast PU films increases with increasing hydrophilicity of polymer chains,[5,9] that is, in the studied samples, with growing DMPA content. Other factors such as the soft-segment type, molecular weight or the chain extender type and functionality also affect the water resistivity of coating materials.[27,34] The effects of BD [PUF A-1 series, Figure 4(a,b)] and DMPA contents [PUF 0.5-B, Figure 4(c)] on the degree of swelling (DS) were investigated on the timescale of hundreds of days.

Figure 4 shows that the initial rate of swelling (up to 5 h) almost does not depend on the sample composition. The mass increase (~3 wt %) at this stage is more likely the result of physical binding of water molecules onto the film surface than the diffusion inside the film. This type of polyurethane–water interaction is highly probable because the hydrophilic ionic groups are regularly distributed within the polyurethane chain and therefore also on the film surface. After 5 h, the rates of swelling of individual samples start to differentiate from each other and depend on the film composition. After 60 h, the maximum differences in the swelling degree reach 10 wt % of water [see Figure 4(a)], which represents almost 100% of the relative swelling. As the ratio of DMPA to PC is kept constant in the PUF A-1 series (see Table I for the compositions), the comparison of curves in Figure 4(a,b) shows that water resistivity of cast films increases with the hard-segment content. As already mentioned, the influence of DMPA content on the water resistivity is antagonistic to that of BD: the resistivity to swelling increases with decreasing DMPA content [Figure 4(c)] which is in accordance with literature data.[35] At low DMPA contents, up to 0.16 mmol g^{-1} (PUF 0.5–0.2 and PUF 0.5–0.4), DS did not exceed 12 wt % within the 16 weeks of conducted measurements. However, for the sample with a high DMPA content (PUF 0.5–1), large DS of 115 wt % was obtained after 16 weeks. It can therefore be concluded that DMPA content of about 0.2 mmol g^{-1} represents a threshold value below which the PU films behave as hydrophobic and highly water resistant materials. Below this the PU films are characterized by relatively high swelling resistivity in comparison to PUDs-based films prepared from isophorone diisocyanates and poly(tetra-methylene adipate glycol), where the percentage swelling in water is in a range from 48 to 92 wt %.[36]

With respect to long time (quasi-equilibrium) swelling properties, the prepared PU films can be divided into three categories: little swelling films (PUF 2–1, PUF 0.5–0.2, and PUF 0.5–0.4) which attain only a low quasi-equilibrium DS of about 10 wt %, medium swelling films (PUF 0.8–1 and PUF 1–1) with intermediate DS about 55 wt % and highly swelling films (PUF 0.5–1) which attain high DS of about 115 wt %. The weight

Table V. Swelling Properties of PU Films

Code PUF A-B	Swelling maximum (wt %)	Swelling after 16 weeks (wt %)	Time for maximum swelling* or quasi-equilibrium	Weight loss by swelling Δw (wt %)
PUF 2-1	8.5	2.2	7 days*	3.9
PUF 1-1	53.7	52.5	12 weeks*	3.4
PUF 0.8-1	58.5	56.5	12 weeks*	4.3
PUF 0.5-1	115.1	115.1	13 weeks	4.1
PUF 0.5-0.4	11.7	11.7	13 weeks	1.2
PUF 0.5-0.2	7.01	7.0	12 weeks	1.2

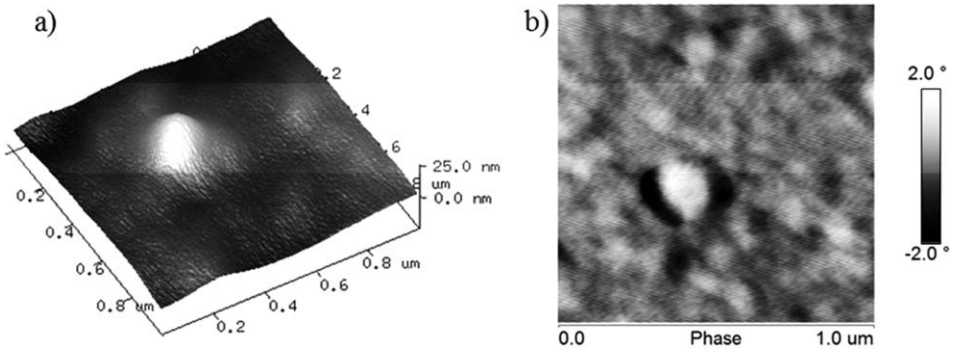

Figure 5. AFM 1 μm × 1 μm images: (a) 3D height, (b) 2D phase of one separated PU nanoparticle from PUD 0.5–0.4.

differences of dry samples before and after swelling were also measured. It was found that they are always fairly low. Lower values (ca. 1 wt %) were obtained for films made from bigger particles while films made from smaller particle lose about 3–4 wt % of the mass, not depending on the attained DS; see Table V, the fifth column.

In the following chapter, the swelling experiments will be further correlated to results of surface analyses (SEM and AFM).

Surface Analysis of PU Films Prepared by PUD Casting

Surface structure belongs to the most important features of films and coatings. Therefore, surface morphology of the PU films was analyzed by two microscopy techniques: atomic force microscopy (AFM) and scanning electron microscopy (SEM). However, before studying the films that are formed by a complex process, during which individual polymer chains from different nanoparticles reorganize and mutually interpenetrate, we studied the deposition of individual nanoparticles on the surface from very diluted solutions.

For the study of the deposition of PU particles on the surface by AFM, we have selected the hydrophilic atomically smooth freshly peeled-out mica surface. The dip-coating technique, consisting in a fast immersion of small mica sheet in a dilute solution followed by fast drying, was used to deposit individual particles. Figure 5 shows one isolated polymer nanoparticle deposited from the diluted aqueous PUD 0.5–0.4 solution. The section analysis of the spherical particle revealed its diameter of about 170 nm. When compared with DLS measurements (particle size 87.6 nm), the size of the deposited particle seems to be larger. This is caused by the pancake deformation of the flexible PU particle upon its deposition on the hydrophilic surface. Because different forces act on the PU nanoparticle in the aqueous dispersion and on the mica surface, it is usually impossible to compare particle sizes obtained from DLS directly. However, it has been shown that AFM is a useful technique for

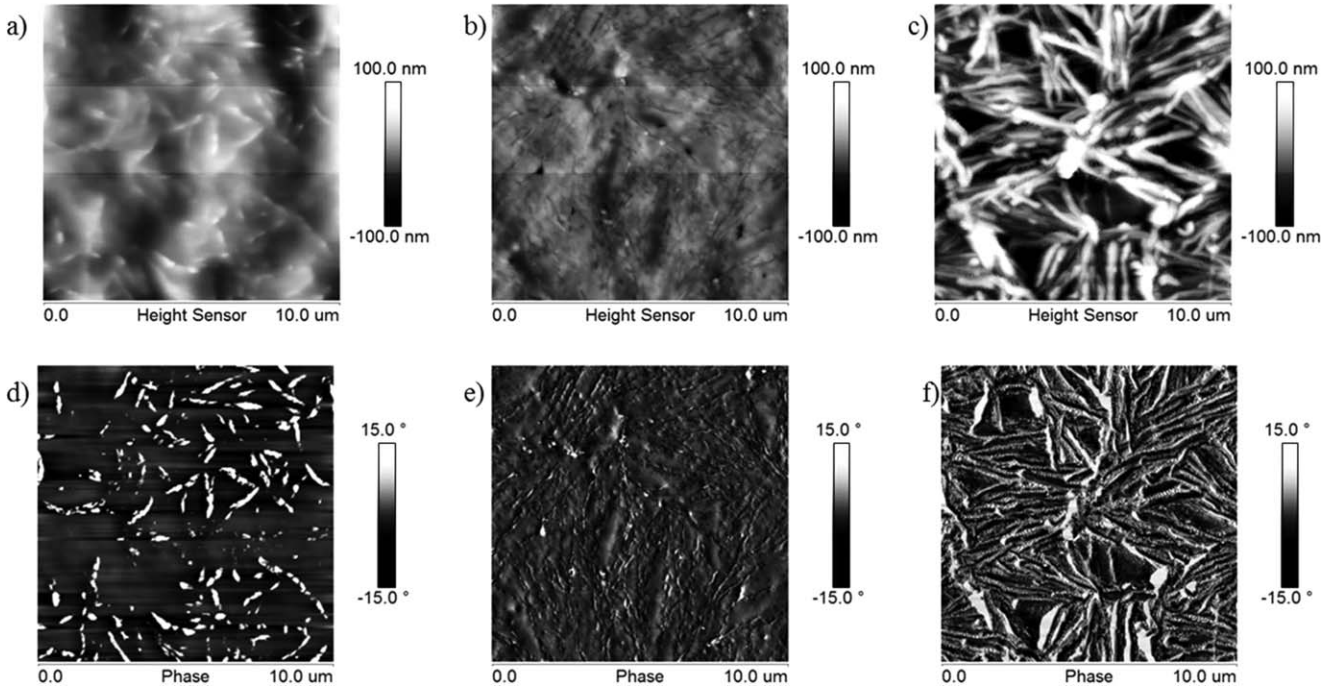

Figure 6. AFM 2D 10 μm × 10 μm (a–c) height, (d–f) phase images of PUF 0.5–0.4 sample prepared by: (a, d) drying at ambient temperature, (b, e) fast water evaporation, (c, d) slow water evaporation and following heating.

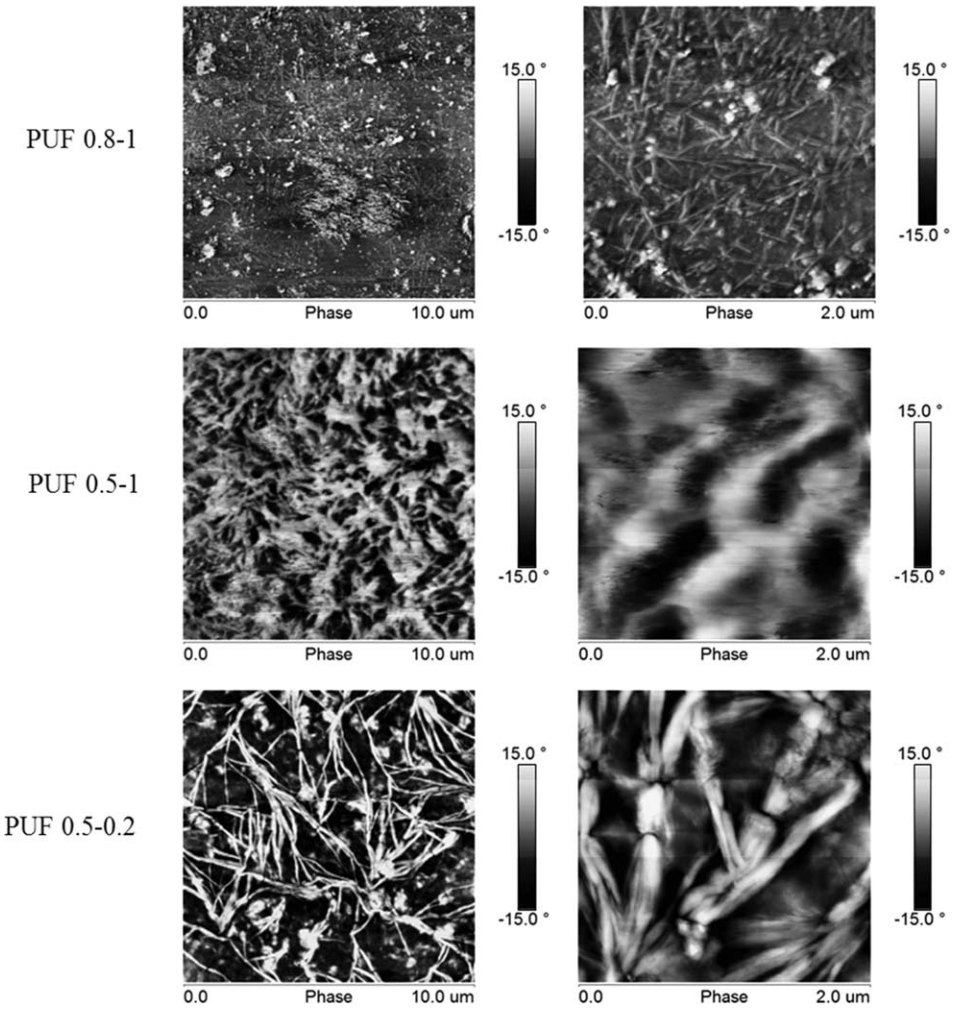

Figure 7. 2D phase AFM images of the cast PUDs films. Scan size 10 μm × 10 μm left, 2 μm × 2 μm right.

investigation of shapes and size distributions of various nanoparticles, including PU nanoparticles.[37,38]

AFM is a powerful tool for checking film surface regularity on the nanometer scale. Three PU samples (PUF 0.5–0.4) of identical composition, but prepared at different rates of water removal during the dispersion thickening and film formation, were analyzed by this method. Figure 6(a,d) shows the height and phase images of films prepared by drying at ambient temperature for 5 days. The slow procedure resulted in randomly oriented rod-like hard domains, which appear at the images as the brightest regions. The results of the second procedure, when the sample was directly heated at 50°C (well above T_g) for 24 h, are presented in Figure 6(b,e). This modification of the preparation procedure, which does not provide enough time for the organization of hard segments within soft phase due to too fast water evaporation, leads to highly disordered morphology of the film surface. To optimize the preparation of films, PUD 0.5–0.4 was dried first at ambient temperature for 5 days and then heated at 50°C ($T_g = -34$°C). Casting the films well above the glass transition temperature at which the polymer chains are highly mobile, results in more regular organization of hard segments. Figure 6(c,f) shows the morphology of the sample prepared by the third method. In this case highly organized and regularly arranged rod-like patterns connected with each other were observed in the AFM image. This indicates that the organization of hard segments depends not only on the rate of water evaporation but also on the casting temperature.

AFM was further used for studies of the effect of different groups content (particularly ionic groups and those that allow the formation of H-bonds) on surface morphology. We found that in all cases, the crystallization of soft segments, described in Differential Scanning Calorimetry section, influences significantly the microphase separation and consequently the surface morphology. Figure 7 compares several selected cast films. Very similar morphology was observed for samples containing different BD contents (series PUF A-1), which suggests that BD did not display significant H-bonding influence on the film morphology. This finding is consistent with DSC data which indicate (e.g., PUF 0.8–1) that hard segments are separated from soft phase depending on the HSC_{BD} concentration (see Table VI). The packing behavior could be caused by the high level of the superstructured organization of hard segments,[39] made

Table VI. Tensile Properties of Cast PU Films Prepared from PUDs of Different Composition: BD—Dependence (PUF A-1 Series) and DMPA—Dependence (PUF 0.5-B Series)

Sample	Young's modulus E (MPa)	Tensile strength σ_b (MPa)	Elongation-at-break ε_b (%)	Energy-to-break (mJ mm^{-3})
PUF 2-1	26.7 ± 0.7	3.7 ± 0.2	288 ± 11	11.2 ± 0.7
PUF 1-1	8.3 ± 0.2	1.4 ± 0.1	208 ± 19	3.5 ± 0.4
PUF 0.8-1	5.9 ± 0.1	1.0 ± 0.1	190 ± 10	2.4 ± 0.2
PUF 0.5-1	3.5 ± 0.1	0.7 ± 0.1	172 ± 7	1.5 ± 0.1
PUF 0.5-0.4	5.5 ± 0.2	1.3 ± 0.1	132 ± 8	1.7 ± 0.1
PUF 0.5-0.2	13.9 ± 0.8	1.8 ± 0.1	128 ± 13	2.4 ± 0.3

from symmetric diisocyanate (HDI) and symmetric BD, together with the high tendency to ordering of carbonate units in soft segments. The study also shows that the content of ionic groups has significant effect on the morphology and microphase separation (observed by AFM). When HSC_{DMPA} content decreases (series 0.5-B), the microphase separation also decreases, which is demonstrated by more homogenous structure of PUD 0.5–1. These observations are consistent with conclusions drawn from DSC results [Figure 3(a)] and support the correctness of the interpretation. Because the charged groups mutually repel, their effect on the compactness of the structure is opposite than that of hydrogen bonds. This may explain more tightly ordered structure of sample containing the lowest HSC_{DMPA} concentration (PUD 0.5–0.2). Similar results were obtained by Sami *et al.*[40] in system without DMPA, where the effect of hydrogen bonds resulted in formation of tightly ordered structure.

2D AFM height images and SEM top images of the surface relief of the PUF 0.5–0.4 cast film are compared in Figure 8. Almost identical magnifications of the images were used in both methods. Both microscopic techniques show similar microstructures where the aforementioned fibril-like structures on the film surface can be easily identified. In both cases, the width of the fibrils is in the range of 80–120 nm. Hollow dips, which retain continuous film surface [Figure 8(c)], can be detected by both techniques. Their presence is presumably the result of water exclusion from the polymer mass during film formation. Swelling experiments (Swelling Behavior section) revealed that this particular sample is very hydrophobic. Gradual water separation results in the formation of stable micrometer-size droplets included in the arising polymer film subsequently evaporated leaving the dip structures on the film surface.

SEM analysis was further used for determination of the effect of the hard-segment concentration on surface film morphology. Microscopic images of cast film surfaces at different BD concentrations (PUF A-1 series)[¶] are shown in Figure 9. Although PUF 0.5–1 [Figure 9(a)] with the lowest BD content exhibits the most homogenous structure, PUF 2–1 with the highest BD content [Figure 9(c)] contains numerous, randomly distributed hollow dips of different sizes. The diameter and average depth of several of the hollow structures were estimated by AFM section analysis and divided into small (1/0.1 μm), medium (2/0.3 μm), and large (5/1 μm) sized features. Number and size of the hollows clearly increase proportionally with increasing BD concentration and therefore the hard-segment content. This can be explained by the fact that samples with higher BD contents easier nucleate in solution. When water is evaporating, particles collide with each other, causing a creation of the porous structure. Conversely, swelling experiments revealed that the hydrophilicity or hydrophobicity of the films has crucial influence on the surface homogeneity of the cast films. The most hydrophilic PUF 0.5–1 has the most homogeneous surface relief while the very hydrophobic PUF 2–1 is distinguished by the highest number of micrometer-size hollow dips. Therefore, formation of the pores may be also caused by more complicated water exclusion process from the hydrophobic polymer mass during film formation. Despite the enlarged porous surface area of PUD 2–1 sample [Figure 9(c)] compared to the other films of the PUF A-1 series, this sample shows the lowest swelling tendency (Table V).

Tensile Properties

The influence of DMPA and BD content on the Young's modulus E, stress-at-break (tensile strength) σ_b, and elongation-at-break ε_b of the cast films were evaluated. The results are summarized in Table VI. As the components used for the PU samples preparation were bifunctional, the resulting cast films were thermoplastic in nature. This is a great advantage because it provides for the reuse and recycling of synthesized samples by various easy available methods, like the injection molding or extrusion. Nevertheless, the absence of chemical cross-lings has a detrimental effect on mechanical properties, which are worse than those of similar chemically cross-linked PU compounds, for example, of those cross-linked by tetrafunctional amines.[35,41]

Two aspects influencing the mechanical properties were investigated: (i) BD concentration (PUF A-1 series) and (ii) the effect of DMPA content (PUF 0.5-B series). Tensile curves of the two series of samples are shown in Figure 10.

The results can be summarized as follows: increasing amount of BD leads to gradual increase of E (Table VI, the second column). This behavior, which has been found in many PU systems,[13,42] is directly related to the hard-segment-promoted increase of sample compactness. Simultaneous increase in tensile strength, elongation at break, and toughness is observed for the

[¶]The unstable dispersion PU 2.5–1 was not used for the film formation.

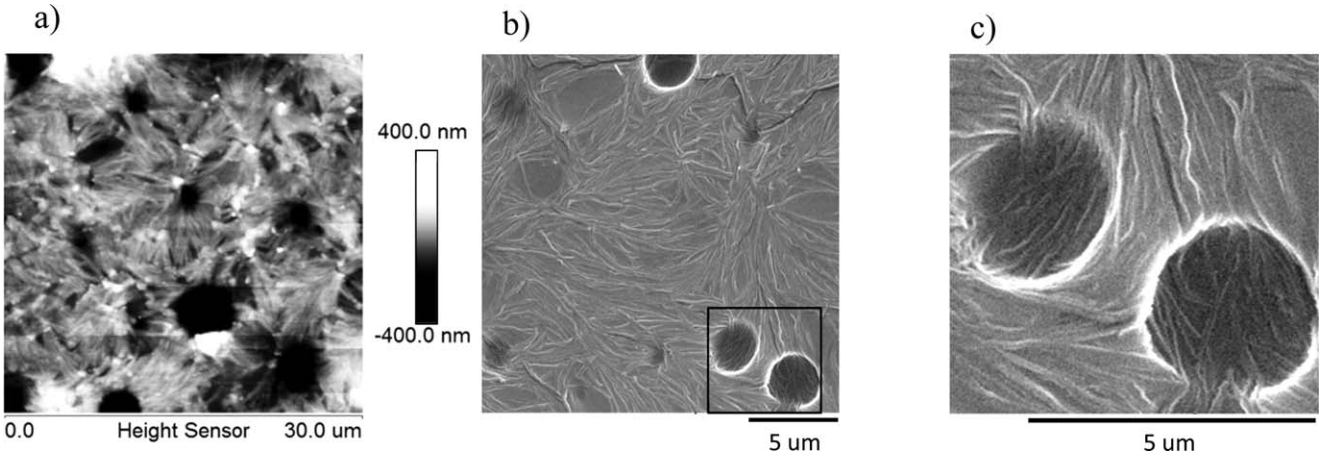

Figure 8. The microstructure of PUF 0.5–0.4: (a) 2D height AFM image (30 μm × 30 μm), (b) SEM image (magnification ×7000), and (c) SEM image (magnification ×30,000).

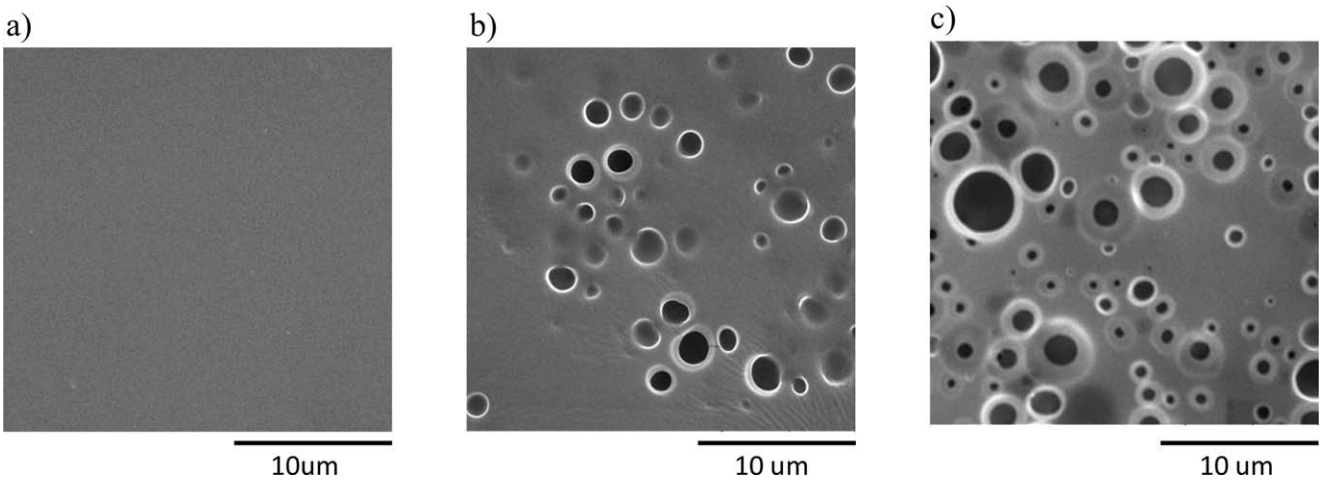

Figure 9. SEM images of PUDs-based films with different BD content (PUF A-1 series): (a) PUF 0.5–1, (b) PUF 1–1, and (c) PUF 2–1 at magnification ×5000.

whole series: PUF A – 1, with the best mechanical properties found for PUF 2 – 1.

The effect of DMPA concentration (PUF 0.5-B series) on the tensile properties is shown in Figure 10(b). Simultaneous increase of E, σ_b, and the energy-to-break and at the same time decrease of ε_b can be seen with the decreasing concentration of the anionic groups (DMPA) [Tables I and III and Figure 10(b)]. The two tensile characteristics, namely σ_b and ε_b, show opposite trends which contradicts the results for films based on both (a) PU dispersions of chemically cross-linked systems (where the

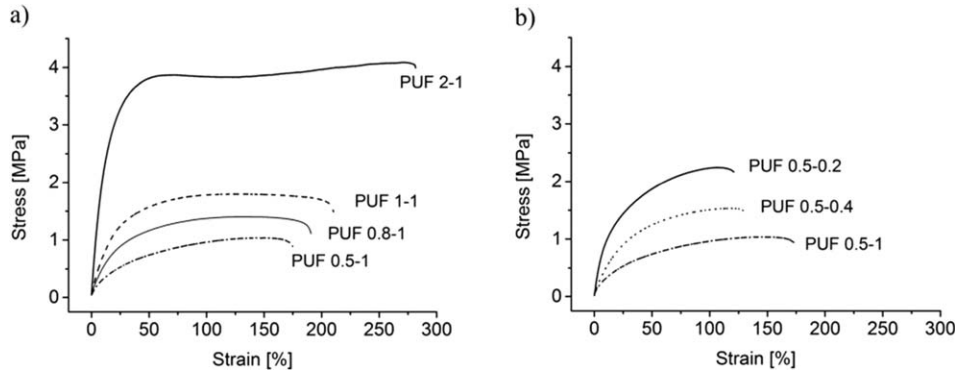

Figure 10. Tensile curves of cast PU films (a) at different BD concentrations (PUF A-1 series), and (b) at different DMPA concentrations (PUF 0.5-B series).

increase of DMPA content resulted in σ_b increase and ε_b decrease[9]) and (b) related starting materials such as PC macrodiol, HDI, and BD prepared by bulk polymerization.[13,43]

The most important factor influencing the PUD composition and average particle size in the PUD 0.5-B series is clearly the DMPA content. It can be assumed that the increase of the anionic group number and also the decrease of average particle size of the dispersions lead to somewhat looser structures, with Coulombic forces overwhelming the hydrogen bonding interactions in the hard segments. All charged nanoparticles are self-assembled entirely from linear PU chains. The packing of the particles and resulting compactness of the films are dependent on the average particle size and their anionic strength. Although smaller, highly charged particles give less tight and less compact materials, bigger and less charged particles form stronger films at low hard-segment contents.

The highest energy-to-break is observed for PUF 2–1 in PUF A-1 and for PUF 0.5–0.2 in the PUF 0.5-B series. Both films are also distinguished by sufficient water resistance (see Swelling Behavior section for details) but they differ in the average size of the dispersion particles (Table III). Both formulations (PUF 2–1 and PUF 0.5–0.2) are excellent candidates for top coating materials which can be applied in both internal and external conditions.

CONCLUSIONS

Stable novel water-borne dispersions based on linear PU chains containing only the aliphatic components such as polycarbonate-based macrodiol, DMPA, HDI, and BD were prepared and characterized. The average particle size (between 45 and 105 nm) decreases with increasing DMPA content, but is only slightly influenced by the amount of chain extender (BD) in the polymer. The absolute values of ζ-potential (between -29 and -65 mV) decrease with ascending DMPA and descending BD contents. The long-term stability tests confirmed that all these dispersions are stable for the minimum period of 1 year. The only exception is the dispersion of the sample with the highest BD content (with the lowest absolute value of ζ-potential -29 mV), the stability of which was found to be limited to 5 months only.

Surface morphology, swelling degree, and tensile properties of the cast films made from polyurethane dispersions were found to depend strongly on the dispersion composition, mainly on the content of the anionic groups as given by DMPA concentration. Three swelling categories were detected: low degree of swelling of about 10 wt %, intermediate with about 55 wt %, and finally high degree of approximately 115 wt %. The surface of films with relatively high (>0.1 mmol g^{-1}) DMPA content shows the self-assembly of particles on the nanometer and micrometer scale arranged into irregular interlined fibril-like structures as detected by AFM. Although the length of fibril-like structure is on the micron unit level, its width is in tens of nanometers. The surface structures and morphologies of individual samples also differ on both the micrometer and millimeter scale depending of the composition, as detected by SEM. The micrometer-size pores are detectable on the surface of hydrophobic PU films, giving a rough design to the material on the micrometer scale. However, on the millimeter level the surface appears relatively regular. Mechanical properties are substantially influenced by the composition of the given dispersions. Tensile strength, elongation-at-break, and energy-to-break increase with increasing BD contents, but increasing DMPA contents leads to higher elongation-at-break but lower tensile strength and energy-to-break. Summarizing the conclusions concerning the functional properties from the practical point of view, samples PUF 0.5–0.2 and especially PUF 2–1 seem the best candidates for the use as internal or external topcoat materials.

ACKNOWLEDGMENTS

The authors wish to thank the financial support of the Grant Agency of the Czech Republic (Czech Science Foundation, project No. 13–06700S).

REFERENCES

1. Brock, T.; Groteklaes, M.; Mischke, P. European Coatings Handbook, Vincentz Verlag: Hannover, **2000**, p 67.
2. Chattopadhyay, D. K.; Raju, K. V. S. N. *Prog. Polym. Sci.* **2000**, *32*, 352.
3. Cakić, S. M.; Stamenković, J. V.; Djordjević, D. M.; Ristić, I. S. *Polym. Deg. Stab.* **2009**, *94*, 2015.
4. Nanda, A. K.; Wicks, D. A.; Madbouly, S. A.; Otaigbe, J. U. *J. Appl. Polym. Sci.* **2005**, *98/6*, 2514.
5. Kim, B. K. *Colloid Polym. Sci.* **1996**, *274*, 599.
6. Cakić, S. M.; Ristić, I. S.; Marinović-Cincović, M.; Špírková, M. *Int. J. Adhes. Adhes.* **2013**, *41*, 132.
7. Król, P. *Prog. Mater Sci.* **2007**, *52*, 915.
8. Chen, T. K.; Chui, J. Y.; Shieh, T. S. *Macromolecules* **1997**, *30*, 5068.
9. Kim, B. K.; Lee, J. C. *Polymer* **1996**, *37*, 469.
10. Lee, D. K.; Tsai, H. B.; Tsai, R. S. *J. Appl. Polym. Sci.* **2006**, *102*, 4419.
11. Nanda, A. K.; Wicks, D. A. *Polymer* **2006**, *47*, 1805.
12. Špírková, M.; Poręba, R.; Pavličević, J.; Kobera, L.; Baldrian, J.; Pekarek, M. *J. Appl. Polym. Sci.* **2012**, *126*, 1016.
13. Poręba, R.; Špírková, M.; Brožová, L.; Lazić, N.; Pavličević, J.; Strachota, A. *J. Appl. Polym. Sci.* **2013**, *127/1*, 329.
14. Noble, K. L. *Prog. Org. Coat.* **1997**, *732*, 131.
15. Delpech, M. C.; Coutinho, F. M. *Polym. Test.* **2000**, *19*, 939.
16. Lee, D. K.; Yang, Z. D.; Tsai, H. B.; Tsai, R. S. *Polym. Eng. Sci.* **2009**, *49*, 2264.
17. Garcia-Pacios, V.; Jofre-Reche, J. A.; Costa, V.; Colera, M.; Martin-Martinez, J. M. *Prog. Org. Coat.* **2013**, *76*, 1484.
18. Cakić, S. M.; Špírková, M.; Ristić, I. S.; B-Simendić, J. K.; M-Cincović, M.; Poręba, R. *Mater. Chem. Phys.* **2013**, *138*, 277.
19. Lee, D. K.; Tsai, H. B.; Yang, Z. D.; Tsai, R. S. *J. Appl. Polym. Sci.* **2012**, *126*, E275.

20. Madbouly, S. A.; Otaigbe, J. U. *Prog. Polym. Sci.* **2009**, *34*, 1283.
21. Garcia-Pacios, V.; Costa, V.; Colera, M.; Martin-Martinez, J. M. *Prog. Org. Coat.* **2011**, *71*, 136.
22. Barrére, M.; Landfester, K. *Macromolecules* **2003**, *36*, 5119.
23. Špírková, M.; Kubín, M.; Dušek, K. *J. Macromol. Sci.* **1987**, *A24*, 1151.
24. Štěpánek, P. *J. Chem. Phys.* **1993**, *99*, 6384.
25. Jakeš, J. *Czech. J. Phys.* **1988**, *38*, 1305.
26. Štěpánek, P.; Koňák, Č. *Polymer* **1984**, *21*, 195.
27. Kim, B. K.; Lee, J. C. *J. Polym. Sci., Part A: Polym. Chem.* **1996**, *34*, 1095.
28. Dobrynin, A. V.; Rubinstein, M. *Prog. Polym. Sci.* **2005**, *30*, 1049.
29. Kelly, C. P.; Cramer, C. P.; Truhlar, D. G. *J. Phys. Chem. B* **2006**, *110*, 16066.
30. Ostolska, I.; Wiśniewska, M. *Colloid Polym. Sci.* **2014**, *292*, 2453.
31. Lee, J.; Kim, M.; Hong, C. K.; Shim, S. E. *Meas. Sci. Technol.* **2007**, *18*, 3707.
32. Dietrich, D.; Keberle, W.; Witt, H. *Angew. Chem. Int. Edit.* **1970**, *9*, 40.
33. Saiani, A.; Rochas, C.; Eeckhaut, G.; Daunch, W. A.; Leenslag, J. W.; Higgins, J. S. *Macromolecules* **2004**, *37*, 1411.
34. Hourston, D. J.; Williams, G.; Satguru, R.; Padget, J. D.; Pears, D. *J. Appl. Polym. Sci.* **1998**, *67*, 1437.
35. Lee, J. S.; Kim, B. K. *Prog. Org. Coat.* **1995**, *25*, 311.
36. Lee, Y. M.; Lee, J. C.; Kim, B. K. *Polymer* **1994**, *35*, 1095.
37. Matějíček, P.; Humpolíčková, J.; Procházka, K.; Tuzar, Z.; Špírková, M.; Hof, M.; Webber, S. E. *J. Phys. Chem.* **2003**, *107*, 8232.
38. Sultan, M.; Islam, A.; Gull, N.; Bhatti, H. N.; Safa, Y. *J. Appl. Polym. Sci.* **2015**, *132*, 41706.
39. Yilgor, I.; Yilgor, E.; Wilkes, G. L. *Polymer* **2015**, *58*, A1.
40. Sami, S.; Yildirim, E.; Yurtsever, M.; Yurtsever, E.; Yilgor, E.; Yilgor, I.; Wilkes, G. L. *Polymer* **2014**, *55*, 4563.
41. Nanda, A. K.; Wicks, D. A.; Madbouly, S. A.; Otaigbe, J. U. *J. Appl. Polym. Sci.* **2005**, *98*, 2514.
42. Korley, L. T. J.; Pate, B. D.; Thomas, E. L.; Hammond, P. T. *Polymer* **2006**, *47*, 3073.
43. Špírková, M.; Pavličević, J.; Strachota, A.; Poręba, R.; Bera, O.; Kaprálková, L.; Baldrian, J.; Šlouf, M.; Lazić, N.; B-Simendić, J. *Eur. Polym. J.* **2011**, *47*, 959.